PHYSICAL REVIEW D VOLUME 14, NUMBER 8 15 OCTOBER 1976

Lattice Hamiltonian results for the spectrum of a (1 + 1)-dimensional asymptotically free field theory*

J. Shigemitsu
Laboratory of Nuclear Studies, Cornell University, Ithaca, New York 14853

S. Elitzur†
Department of Physics, Tel Aviv University, Ramat Aviv, Israel

(Received 12 May 1976)

Using lattice Hamiltonian methods, we investigate the spectrum of an asymptotically free field theory in 1 + 1 dimensions, the SU(N) Thirring model. Lattice perturbation calculations are carried out to fourth order in the expansion parameter $1/g^2$. These calculations are extrapolated to the continuum (lattice spacing$\to$0) using Padé approximants and are compared with the WKB results of Dashen, Hasslacher, and Neveu. Good agreement is found in many cases. The reliability of the Padé extrapolation method is studied by comparing several strong-coupling spectrum calculations with approximate mean-field calculations of the same quantities. The results are very encouraging.

I. INTRODUCTION

This paper reports on the application of lattice Hamiltonian methods[1-3] to study the SU(N) Thirring model,[4] a model in 1 + 1 dimensions with N species of self-interacting fermions:

$$\mathcal{L} = \sum_{\alpha=1}^{N} i\bar{\psi}_\alpha \not{\partial} \psi_\alpha + \frac{g^2}{2}\left(\sum_{\alpha=1}^{N} \bar{\psi}_\alpha \psi_\alpha\right)^2 . \tag{1.1}$$

The model is renormalizable and asymptotically free. Gross and Neveu[5] have shown that it is also a theory in which discrete γ_5 symmetry is dynamically broken. In the true ground state $\bar{\psi}\psi$ acquires a nonvanishing vacuum expectation value and the fermions develop a mass dynamically.

More recently Dashen, Hasslacher, and Neveu[6] (DHN), applying semiclassical WKB methods, have discovered a rich spectrum in the model. In addition to kinklike solutions they find a large number of less exotic objects, which they say are likely to have their counterparts in four-dimensional theories. These latter solutions correspond to the fundamental fermion, to fermion-fermion, antifermion-antifermion, and fermion-antifermion bound states, and to further multiparticle states.

Calculating the mass spectrum of an asymptotically free quantum field theory is also a major goal of the lattice Hamiltonian methods. Since calculations in 3 + 1 dimensions are already underway, it is important to test these methods, within a simple one-dimensional setting, where results obtained by more conventional means are available. We have attempted to perform such a test and the results are presented in this paper. In brief, we have calculated particle masses to fourth order in strong-coupling perturbation theory, formulated on a lattice. Upon extrapolating to the continuum limit, we have found good agreement with the results of DHN.

In order to clarify and justify the previous statement, we must discuss our method for passing from a lattice theory to the continuum limit, within the context of an asymptotically free model. We must also demonstrate asymptotic freedom starting directly from a lattice Hamiltonian.

To study these points we took up the ideas of a recent paper by Zee,[7] who uses a gap equation,[8] familiar from Bardeen-Cooper-Schrieffer (BCS) mean-field theory, to find a relation between the effective coupling constant "$g^2(a)$" and the lattice spacing "a". He shows that in the large-N limit, $g^2(a) \propto a\Delta$ for large "$a\Delta$," and $g^2(a) \propto -1/\ln a\Delta$ for small $a\Delta$, where Δ = gap. Analyzing the gap equation in detail, we have found that Zee's results remain good approximations for N values ≥ 4. Furthermore, identifying the gap Δ with the dynamically produced fermion mass, M_F, the large-g^2 limit of the gap equation gives the exact value for $(2aM_F)_0$, our zeroth-order strong-coupling result in configuration space. At the weak coupling end, the gap equation reproduces, for large N, the results of Gross and Neveu,[5] i.e., the correct lowest-order contribution to the Callan-Symanzik β function.

Thus, the pairing approximation works very well for this simple theory at both the strong- and weak-coupling limits. Therefore, we are inclined to believe that it gives us a fairly accurate curve of $g^2(a)$ vs a over the whole range of g^2, from zero to infinity. The plotted curve (see Appendix) indicates then that the cutoff lattice theory tends smoothly toward the continuum limit as $g^2 \to 0$. Such a result is crucial to the success of the lattice Hamiltonian approach, since it means that a singularity-free extrapolation from the strongly

coupled lattice theory to the asymptotically free continuum theory is possible.

Having learned this from our investigations in momentum space, we next must implement this limiting procedure within strong-coupling perturbation theory which employs the expansion parameter $x(a) \equiv 2/g^2(a)$. As we will see later, fourth-order lattice calculations leave us with a Taylor series for mass ratios of the form

$$\frac{M_1}{M_2} = A + B\left(\frac{2}{g^2(a)}\right)^2 + C\left(\frac{2}{g^2(a)}\right)^4 \qquad (1.2)$$

(A, B, C are constants).

Now we have found that to go to the continuum limit we must let $g^2 \to 0$, where the Taylor series of Eq. (1.2) does not converge. Therefore, we need a method to extrapolate the series of Eq. (1.2) outside its radius of convergence. Following Ref. 3, we have chosen to replace the Taylor series of Eq. (1.2) by a Padé approximant[9] before taking the continuum limit. In particular, Eq. (1.2) is replaced by its [1, 1] Padé approximant

$$\frac{M_1}{M_2} = \frac{A + Dx^2}{1 + Ex^2}, \quad x = 2/g^2 . \qquad (1.3)$$

The continuum limit can now be trivially taken using Eq. (1.3).

This extrapolation procedure, replacing a Taylor series by a Padé approximant, is not new. It has been successfully employed in the study of critical phenomena. There is a close analogy between high-temperature expansions and critical behavior on the one hand, and strong-coupling expansions and the continuum limit on the other. The reader should consult Ref. 9 for further discussion, and (we hope) convince himself that this extrapolation method is worth investigating.

We have chosen the diagonal [1, 1] Padé approximant in Eq. (1.3) since it incorporates the boundary condition that mass ratios such as Eq. (1.3) go toward a constant as $g^2 \to 0$. As DHN[6] point out, this is the correct boundary condition to use when one is dealing with an asymptotically free theory with only one coupling constant and with dynamical symmetry breaking.[10]

We calculated Eq. (1.3) for the ratios of two-particle bound-state masses to the fermion mass, and for the ratios of masses to $g\sigma \equiv -g^2\langle \bar{\psi}\psi \rangle_{\text{vac}}$. Upon taking the limit $g^2 \to 0$ we find good numerical agreement with DHN. Citing one example, for the fermion-fermion bound-state mass, M_{FF}, we obtain in the continuum limit $M_{FF}/g\sigma = 1.937$ for $N = 8$ compared with $(M_{FF}/g\sigma)_{\text{DHN}} = 1.949$. For $N = 20$ we have $M_{FF}/g\sigma = 1.991$ whereas $(M_{FF}/g\sigma)_{\text{DHN}} = 1.992$.

One can test the reliability of the limiting procedure adopted here by applying it to the fermion mass. On the one hand, there is the gap equation telling us how $2aM_F$ should behave as one moves away from the strong-coupling domain. Can one retrieve this curve using fourth-order strong-coupling results and Padé approximants? Alternatively, can the asymptotically free character of the theory be discovered from the strong-coupling expansion? In the strong-coupling limit $2a\Delta$, $2aM_F$, and $g\sigma$ depend linearly on $g^2(a)$. We have compared the deviations from this linear behavior of the gap, $2a\Delta$, as one approaches the weak-coupling domain, with the deviations from the linear behavior of the [1, 1] Padé approximants for $2aM_F$ and $g\sigma$. We observe numerical agreement among the three curves from g^2 of infinity to g^2 of order $\sim 1/N$.

We find it very encouraging that a wide range of g^2 can be covered by doing only fourth-order strong-coupling perturbation calculations. It is, of course, the great hope that, even in (3 + 1)-dimensional theories, low-order lattice calculations will give reliable results for masses of low-lying states, when extrapolated appropriately to the continuum.

This paper is organized into four remaining sections. Section II sets up the SU(N) Thirring model Hamiltonian on a lattice. The potential energy becomes the unperturbed Hamiltonian H_0 in the strong-coupling approximation. The kinetic energy is put in as a perturbation. We will see that discrete γ_5 symmetry is broken in the lattice theory.

In Sec. III the spectrum of H_0 is obtained and particle states are defined. The zeroth-order spectrum already exhibits features of the DHN spectrum. Section IV discusses the perturbation calculations. Graphs will be introduced and a few examples from second- and fourth-order calculations will be explained. In Sec. V we will take the results of Secs. II–IV, results that were obtained at some fixed lattice spacing a, and make an extrapolation to the continuum. The "continuum values" are then compared with the DHN results. We have also included, as an appendix, our analysis of the gap equation.

II. THE LATTICE HAMILTONIAN

The continuum Hamiltonian for the SU(N) Thirring model is

$$H_c = \int dz \left[\sum_{\alpha=1}^{N} (-i\bar{\psi}^c_\alpha \gamma_1 \partial_z \psi^c_\alpha) - \frac{g^2}{2}\left(\sum_{\alpha=1}^{N} \bar{\psi}^c_\alpha \psi^c_\alpha \right)^2 \right] , \qquad (2.1)$$

where "c" denotes "continuum." The γ matrices employed throughout this paper are

$$\gamma_0=\sigma_3\,,\quad \gamma_1=i\sigma_2\,,\quad \gamma_5=\sigma_1\,.$$

We shall follow Ref. 3 in putting fermion fields on a lattice. We work on a finite lattice with L lattice sites and lattice spacing a, and impose periodic boundary conditions on the fields. At each lattice site l one introduces N one-component fermion fields $\phi_\alpha(l)$ $(\alpha=1,2,\ldots,N)$ (see Ref. 11) obeying

$$\begin{aligned}&\{\phi_\alpha^\dagger(l),\phi_{\alpha'}(l')\}=\delta_{l,l'}\,\delta_{\alpha,\alpha'}\,,\\&\{\phi_\alpha^\dagger(l),\phi_{\alpha'}^\dagger(l')\}=\{\phi_\alpha(l),\phi_{\alpha'}(l')\}=0\,,\end{aligned}\tag{2.2}$$

and

$$\phi_\alpha(l+L)=\phi_\alpha(l)\,.\tag{2.3}$$

These fields have been rescaled by $(2a)^{1/2}$ and are dimensionless. The correspondence between the ϕ fields and the more familiar two-component spinors

$$\begin{pmatrix}\psi_\alpha^1\\ \psi_\alpha^2\end{pmatrix}$$

is the following:

$$\begin{pmatrix}\psi_\alpha^1\\ \psi_\alpha^2\end{pmatrix}\to\begin{pmatrix}\phi_\alpha\ (\text{even site})\\ \phi_\alpha\ (\text{odd site})\end{pmatrix}\,.\tag{2.4}$$

Perhaps the illustration given in Table I will be helpful.

Comparing the intermediate stage and the one-component fields, one sees that there are two ways of interpreting (2.4),

$$\begin{pmatrix}\psi_\alpha^1(2j)\\ \psi_\alpha^2(2j)\end{pmatrix}\to\begin{pmatrix}\phi_\alpha(2j)\\ \phi_\alpha(2j-1)\end{pmatrix}\tag{2.5a}$$

or

$$\begin{pmatrix}\psi_\alpha^1(2j)\\ \psi_\alpha^2(2j)\end{pmatrix}\to\begin{pmatrix}\phi_\alpha(2j)\\ \phi_\alpha(2j+1)\end{pmatrix}\,.\tag{2.5b}$$

In going from continuum expressions to their lattice counterparts, symmetric continuum operators were symmetrized with respect to the two possibilities (2.5a) and (2.5b), in order to preserve left-right symmetry even on the lattice.

As an example take the potential energy term in (2.1)

TABLE I. Correspondence between continuum expressions and their lattice counterparts.

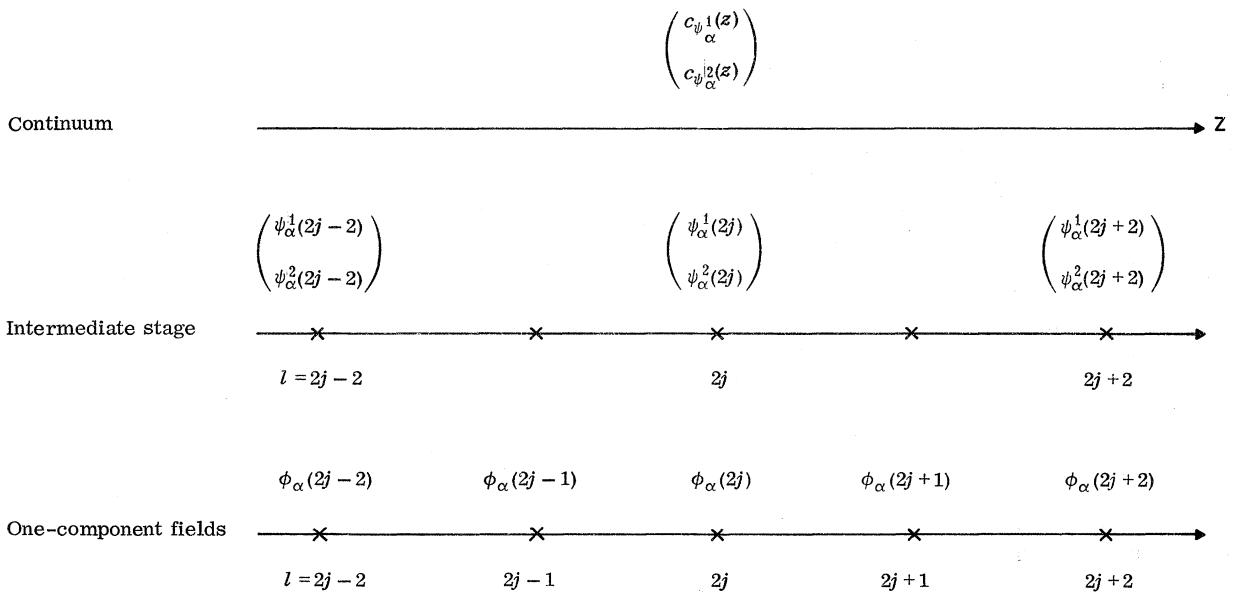

$$\int dz\left(\sum_{\alpha=1}^{N}\bar{\psi}_\alpha^c\psi_\alpha^c\right)^2$$

$$\to 2a\sum_{j=1}^{L/2}\frac{1}{2}\left\{\frac{1}{(2a)^2}\left[\sum_\alpha\left(\phi_\alpha^\dagger(2j)\phi_\alpha(2j)-\phi_\alpha^\dagger(2j-1)\phi_\alpha(2j-1)\right)\right]^2\right.$$
$$\left.+\frac{1}{(2a)^2}\left[\sum_\alpha\left(\phi_\alpha^\dagger(2j)\phi_\alpha(2j)-\phi_\alpha^\dagger(2j+1)\phi_\alpha(2j+1)\right)\right]^2\right\}$$
$$=\frac{1}{4a}\sum_{j=1}^{L/2}\sum_\alpha^N\sum_\beta^N\{2(\phi_\alpha^\dagger(2j)\phi_\alpha(2j))(\phi_\beta^\dagger(2j)\phi_\beta(2j))+(\phi_\alpha^\dagger(2j-1)\phi_\alpha(2j-1))(\phi_\beta^\dagger(2j-1)\phi_\beta(2j-1))$$
$$+(\phi_\alpha^\dagger(2j+1)\phi_\alpha(2j+1))(\phi_\beta^\dagger(2j+1)\phi_\beta(2j+1))-2(\phi_\alpha^\dagger(2j)\phi_\alpha(2j))(\phi_\beta^\dagger(2j-1)\phi_\beta(2j-1))$$
$$-2(\phi_\alpha^\dagger(2j+1)\phi_\alpha(2j+1))(\phi_\beta^\dagger(2j)\phi_\beta(2j))\}$$
$$=\frac{1}{2a}\sum_\alpha^N\sum_\beta^N\left\{\sum_{l=\text{even}}+\sum_{l=\text{odd}}\right\}[(\phi_\alpha^\dagger(l)\phi_\alpha(l))(\phi_\beta^\dagger(l)\phi_\beta(l))-(\phi_\alpha^\dagger(l)\phi_\alpha(l))(\phi_\beta^\dagger(l+1)\phi_\beta(l+1))]\,.$$

So

$$H_{\text{pot}}=-\frac{g^2}{4a}\sum_{l=1}^{L}\sum_\alpha^N\sum_\beta^N\{(\phi_\alpha^\dagger(l)\phi_\alpha(l))(\phi_\beta^\dagger(l)\phi_\beta(l))-(\phi_\alpha^\dagger(l)\phi_\alpha(l))(\phi_\beta^\dagger(l+1)\phi_\beta(l+1))\}\,. \tag{2.6}$$

The quick way to obtain the lattice kinetic energy is to write down an expression which gives the correct free Dirac equation in the continuum limit. Take

$$H_{\text{kin}}=\frac{i}{2a}\sum_{l=1}^{L}\sum_{\alpha=1}^{N}\phi_\alpha^\dagger(l)(\phi_\alpha(l-1)-\phi_\alpha(l+1))\,. \tag{2.7}$$

Using the Heisenberg equation of motion $i\partial_t\phi=[\phi,H]$ and (2.2) one sees that for $H=H_{\text{kin}}$

$$i\partial_t\phi_\alpha(l)=-\frac{i}{2a}(\phi_\alpha(l+1)-\phi_\alpha(l-1))\,. \tag{2.8}$$

From (2.8) one can write

$$i\gamma_0\partial_t\begin{pmatrix}\phi_\alpha(2j)\\ \phi_\alpha(2j-1)\end{pmatrix}=\frac{-i}{2a}\gamma_1\left\{\begin{pmatrix}\phi_\alpha(2j)\\ \phi_\alpha(2j+1)\end{pmatrix}-\begin{pmatrix}\phi_\alpha(2j-2)\\ \phi_\alpha(2j-1)\end{pmatrix}\right\},$$

which reduces to the free Dirac equation in the continuum limit. So we shall take (2.7) to be the lattice equivalent to the kinetic energy term in (2.1). Collecting the two terms our lattice Hamiltonian becomes

$$H=H_{\text{pot}}+H_{\text{kin}}\,,$$

$$H_{\text{pot}}=-\frac{g^2}{4a}\sum_{l=1}^{L}\sum_\alpha^N\sum_\beta^N\{(\phi_\alpha^\dagger(l)\phi_\alpha(l))(\phi_\beta^\dagger(l)\phi_\beta(l))-(\phi_\alpha^\dagger(l)\phi_\alpha(l))(\phi_\beta^\dagger(l+1)\phi_\beta(l+1))\}\,, \tag{2.9}$$

$$H_{\text{kin}}=\frac{i}{2a}\sum_{l=1}^{L}\sum_{\alpha=1}^{N}\phi_\alpha^\dagger(l)(\phi_\alpha(l-1)-\phi_\alpha(l+1))\,.$$

Other operators of interest are as follows:

$$\text{scalar: }\sum_\alpha\int dz\,\bar{\psi}_\alpha^c\psi_\alpha^c\to 2a\sum_{j=1}^{L/2}\sum_\alpha^N\frac{1}{2a}\{\phi_\alpha^\dagger(2j)\phi_\alpha(2j)-\phi_\alpha^\dagger(2j-1)\phi_\alpha(2j-1)\}$$
$$=\sum_{l=1}^{L}\sum_\alpha^N(-1)^l\,\phi_\alpha^\dagger(l)\phi_\alpha(l)\,. \tag{2.10}$$

Here it was not necessary to symmetrize since starting from either (2.5a) or (2.5b) one obtains the same

result (2.10):

$$\text{fermion number: } \sum_{\alpha} \int dz\, \psi^{c\dagger}_{\alpha} \psi^{c}_{\alpha} \to \sum_{l=1}^{L} \sum_{\alpha}^{N} \phi^{\dagger}_{\alpha}(l) \phi_{\alpha}(l) \equiv Q\,. \tag{2.11}$$

In the strong-coupling approximation H_{pot} of Eq. (2.9) becomes the unperturbed Hamiltonian H_0. Our first task will be to find its eigenvalues. The rest of this section is devoted to finding a representation for the ϕ fields, in which this can be accomplished most easily, without making the perturbation term H_{kin} too complicated at the same time.

First we shall perform a Jordan-Wigner[12] transformation and write the fermion fields in terms of spin operators. The transformation is

$$\begin{aligned}
\phi_{\alpha}(l) &= (i\sigma^{z}_{1}(1))(i\sigma^{z}_{2}(1)) \cdots (i\sigma^{z}_{\alpha-1}(l))\sigma^{-}_{\alpha}(l) \\
&= (i)^{N(l-1)} (i)^{\alpha-1} \sigma^{z}_{1}(1) \cdots \sigma^{z}_{\alpha-1}(l) \sigma^{-}_{\alpha}(l)\,, \\
\phi^{\dagger}_{\alpha}(l) &= (-i)^{N(l-1)} (-i)^{\alpha-1} \sigma^{z}_{1}(1) \cdots \sigma^{z}_{\alpha-1}(l) \sigma^{+}_{\alpha}(l)\,,
\end{aligned} \tag{2.12}$$

where $\sigma^{\pm} = \frac{1}{2}(\sigma^{x} \pm i\sigma^{y})$.

The transformation (2.12) preserves the anticommutation relations for the ϕ fields, but has the advantage that one then deals with operators $\sigma^{i}_{\alpha}(l)$ that commute at different sites and for different species.

Applying this transformation to the lattice Hamiltonian (2.9) one has

$$H_{\text{pot}} = \frac{g^2}{16a} \sum_{l=1}^{L} \sum_{\alpha,\beta}^{N} \{\sigma^{z}_{\alpha}(l)\sigma^{z}_{\beta}(l+1) - \sigma^{z}_{\alpha}(l)\sigma^{z}_{\beta}(l)\}\,, \tag{2.13}$$

$$H_{\text{kin}} = \frac{(i)^{N+1}}{2a} \sum_{l=1}^{L} \sum_{\alpha}^{N} \{\sigma^{+}_{\alpha}(l)\sigma^{-}_{\alpha}(l+1) - (-1)^{N}\sigma^{+}_{\alpha}(l+1)\sigma^{-}_{\alpha}(l)\}\sigma^{z}_{\alpha+1}(l)\sigma^{z}_{\alpha+2}(l) \cdots \sigma^{z}_{\alpha-1}(l+1)\,. \tag{2.14}$$

H_{pot} has become very much more tractable in this representation, but at the cost of having products of σ^{z}'s in the perturbation term. These will cause no trouble if they act on eigenstates of σ^{z} with eigenvalue +1. So what one should try to do is to arrange things in such a way that the vacuum has all spins pointing up. It is possible to accomplish this by performing yet another transformation[13]:

$$\left.\begin{aligned}
&\sigma^{+}_{\alpha}(l) \to \sigma^{-}_{\alpha}(l) \\
&\sigma^{-}_{\alpha}(l) \to \sigma^{+}_{\alpha}(l) \\
&\sigma^{z}_{\alpha}(l) \to -\sigma^{z}_{\alpha}(l)
\end{aligned}\right\} \text{for } l = \text{even}\,, \tag{2.15a}$$

$$\sigma_{\alpha}(l) \text{ unchanged for } l = \text{odd}\,. \tag{2.15b}$$

Substituting (2.15) into (2.13) and (2.14) and dividing by $g^2/4a$ one obtains

$$W \equiv \frac{4a}{g^2} H = W_0 + xV\,, \tag{2.16}$$

with

$$W_0 = -\tfrac{1}{4} \sum_{l}^{L} \sum_{\alpha,\beta}^{N} \{\sigma^{z}_{\alpha}(l)\sigma^{z}_{\beta}(l) + \sigma^{z}_{\alpha}(l)\sigma^{z}_{\beta}(l+1)\}\,, \tag{2.17}$$

$$V = -(i)^{N+1} \sum_{l}^{L} \sum_{\alpha}^{N} \{\sigma^{+}_{\alpha}(l)\sigma^{+}_{\alpha}(l+1) + (-1)^{N+1}\sigma^{-}_{\alpha}(l)\sigma^{-}_{\alpha}(l+1)\}(-1)^{\alpha}\sigma^{z}_{\alpha+1}(l) \cdots \sigma^{z}_{\alpha-1}(l+1)\,, \tag{2.18}$$

$x = 2/g^2$.

In this representation (2.10) and (2.11) take the form

$$\text{scalar: } \sum_{\alpha}^{N} \int \bar{\psi}^{c}_{\alpha} \psi^{c}_{\alpha}\, dz \to -\tfrac{1}{2} \sum_{l}^{L} \sum_{\alpha=1}^{N} \sigma^{z}_{\alpha}(l)\,, \tag{2.19}$$

$$\text{fermion number: } Q=-\tfrac{1}{2}\sum_{l}^{L}\sum_{\alpha}^{N}(-1)^{l}\sigma_{\alpha}^{z}(l)=\sum_{\alpha}^{N}Q_{\alpha},\quad Q_{\alpha}=-\tfrac{1}{2}\sum_{l}^{L}(-1)^{l}\sigma_{\alpha}^{z}(l)\,. \tag{2.20}$$

Also

$$\sum_{\alpha}^{N}\bar{\psi}_{\alpha}^{c}\psi_{\alpha}^{c}\Big|_{\text{at } x=2ja}\rightarrow-\frac{1}{8a}\sum_{\alpha=1}^{N}\{2\sigma_{\alpha}^{z}(2j)+\sigma_{\alpha}^{z}(2j+1)+\sigma_{\alpha}^{z}(2j-1)\}\,. \tag{2.21}$$

Is the ground state of W_0, Eq. (2.17), the all-spins-up configuration? The first term in W_0 requires the orientation of the spins at each given lattice site to be the same for all species. Then the second term fixes the spins at two adjacent sites to be parallel. So by considering (2.17) alone one finds a two-fold degeneracy for the ground state, either all spins up or all spins down. We shall pick our ground state by imagining that a small-mass term has been turned on, minimizing the ground-state energy and then letting the mass go to zero. A look at Eq. (2.19) tells us that one will be left with the all-spins-up configuration. We shall call this state our vacuum and all eigenvalues of W_0 will be measured relative to this state.

Taking the expectation value of (2.21) in the vacuum state defined above, one has

$$\langle\bar{\psi}_c\psi_c\rangle_0=-\frac{N}{2a}\neq 0\,, \tag{2.22}$$

and one sees that by choosing one out of the two possible vacua, spontaneous symmetry breaking is introduced into the lattice theory.[7] Recalling that $\langle\bar{\psi}_c\psi_c\rangle_0\neq 0$ also in the continuum theory, one can now hope that the lattice theory has been set up in the "correct phase," and that a singularity-free extrapolation to the continuum is possible.

In this section we have obtained the lattice Hamiltonian (2.16), which is to replace Eq. (2.1) of the continuum theory. We find that in the strong-coupling approximation, the zeroth-order vacuum exhibits spontaneous symmetry breaking. In the next two sections we will analyze the system characterized by the lattice Hamiltonian. In Sec. V the connection with the continuum theory will be reestablished.

III. THE SPECTRUM OF W_0 AND "PARTICLE STATES"

Since the vacuum has all spins pointing up, excited states in our representation will correspond to configurations with a certain number of spins flipped down. At each lattice site it is possible to flip from one up to N spins. To find the eigenvalues of W_0 for such states consider separately the contributions coming from the first term in (2.17) which only involves spins at a given lattice site, and from the second term, which is a nearest-neighbor coupling term. Both terms have two independent sums over all species.

Let P_l stand for the number of spins that have been flipped on site l. For each l the first term in W_0, $-\frac{1}{4}\sum_{\alpha,\beta}^{N}\sigma_{\alpha}^{z}(l)\sigma_{\beta}^{z}(l)$, will contribute

$$P_l(N-P_l)\,. \tag{3.1}$$

Equation (3.1) is easily obtained by noting that the sum $\sum_{\alpha,\beta}^{N}$ is just a sum over a certain number n^+ of $(+1)$'s and n^- of (-1)'s, with $n^++n^-=N^2$. From Fig. 1(a) one has

$$-\tfrac{1}{4}\sum_{\alpha,\beta}^{N}\sigma_{\alpha}^{z}(l)\sigma_{\beta}^{z}(l)=-\tfrac{1}{4}[P_l{}^2+(N-P_l)^2-2P_l(N-P_l)]$$
$$=-\tfrac{1}{4}(N^2+4P_l{}^2-4NP_l)\,.$$

Subtracting the vacuum value $-N^2/4$, (3.1) results. Using the same method for the nearest-neighbor coupling term, Fig. 1(b) gives

$$-\tfrac{1}{4}\sum_{\alpha,\beta}^{N}\sigma_{\alpha}^{z}(l)\sigma_{\beta}^{z}(l+1)+\frac{N^2}{4}$$
$$=-\tfrac{1}{4}[(N-P_l)(N-P_{l+1})+P_lP_{l+1}-(N-P_l)P_{l+1}$$
$$-(N-P_{l+1})P_l]+\frac{N^2}{4}$$
$$=\frac{(P_l+P_{l+1})}{2}N-P_l\cdot P_{l+1}\,. \tag{3.2}$$

Adding (3.1) and (3.2) and summing over all lattice

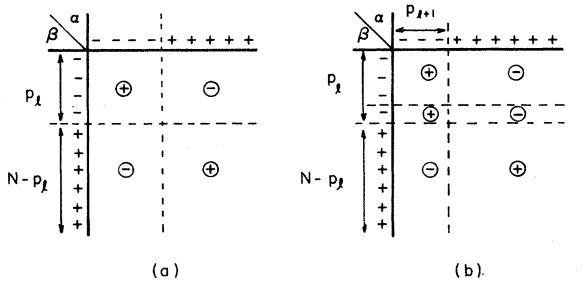

FIG. 1. Contributions to the eigenvalues of W_0 from (a) the first term and (b) the second term in Eq. (2.17).

sites

$$\langle\{P_l\}|W_0|\{P_l\}\rangle = \sum_l^L (2P_l N - P_l^2 - P_l \cdot P_{l+1})$$
$$= 2nN - B, \tag{3.3}$$

where

$$n = \sum_l^L P_l = \text{total number of spins flipped},$$
$$B = \sum_l^L (P_l^2 + P_l P_{l+1}), \tag{3.4}$$

With these definitions the expectation values of H_0 become

$$E_0(n,B) \equiv \langle\{P_l\}|H_0|\{P_l\}\rangle = \frac{g^2}{2a}\left(nN - \frac{B}{2}\right),$$

or, upon introducing

$$\sigma_0 \equiv -g\langle\bar{\psi}^c \psi^c\rangle_0 = \frac{gN}{2a}, \tag{3.5}$$

one can write

$$\frac{E_0(n,B)}{g\sigma_0} = \left(n - \frac{B}{2N}\right). \tag{3.6}$$

Equation (3.6) has been plotted in Fig. 2 for $N=4$ and $N=8$. The dotted lines give the DHN values, where their "principal quantum number n" has been identified with our n of (3.4),

$$\left(\frac{E(n)}{g\sigma}\right)_{\text{DHN}} = \frac{2N}{\pi}\sin\left(n\frac{\pi}{2N}\right) \quad (n=1,2,\ldots<N). \tag{3.7}$$

The levels in our spectrum with an asterisk correspond to states where all n excitations occur either at one lattice site or on two adjacent sites. They are the lowest-lying states for given n, and we interpret them as bound states (for $n<N$). For given n and N the sum of the degeneracies of these bound states is

$${}_N C_n + {}_N C_{n-1}\,{}_N C_1 + \cdots + {}_N C_1\,{}_N C_{n-1} + {}_N C_n = {}_{2N}C_n$$
$$= \frac{(2N)!}{(2N-n)!n!}.$$

These states constitute the lowest-lying O($2N$) multiplet the DHN find in their spectrum (the $n_0 = n$ multiplets in their notation).

From Fig. 2 one sees that there can be degeneracies among levels with different n values (when n becomes equal to or greater than N this will always be the case), and in such a situation a straightforward perturbation calculation is no longer possible. As long as one is interested only in one- and two-particle states, setting $N \geq 4$ will eliminate this difficulty, and for the perturbation calculations of the next section we will always assume that $N \geq 4$ holds.

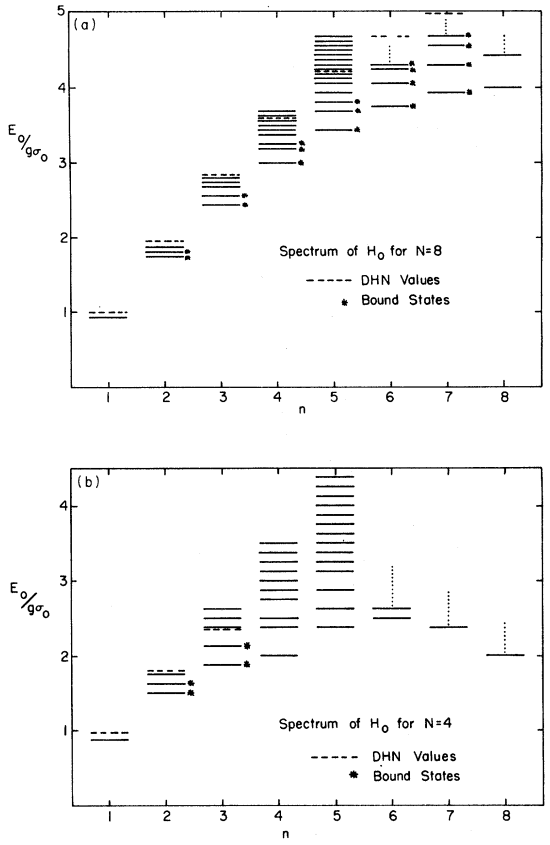

FIG. 2. The spectrum of H_0 for (a) $N=8$ and (b) $N=4$. "n" is the number of excitations.

The total Hamiltonian commutes with the fermion number $Q = \sum_\alpha Q_\alpha$ and with each individual Q_α. We will label particle states by their species number. The state $|l,\rho\rangle \equiv \sigma_\rho^-(l)|\Omega\rangle$ satisfies

$$W_0|l,\rho\rangle = (2N-1)|l,\rho\rangle,$$
$$Q|l,\rho\rangle = (-1)^l|l,\rho\rangle, \tag{3.8}$$
$$Q_\alpha|l,\rho\rangle = (-1)^l\delta_{\alpha,\rho}|l,\rho\rangle.$$

Recalling that $\phi_{(l=\text{even})}$ corresponds to the upper component and $\phi_{(l=\text{odd})}$ to the lower component of a Dirac spinor, we will identify $|l,\rho\rangle$ with a "fermion state" for $l=$ even ($Q=+1$), and with an "antifermion state" for $l=$ odd ($Q=-1$).

Making translationally invariant combinations (zero-momentum states) one has

$$|\rho\rangle_{\text{fermion}} = \left(\frac{2}{L}\right)^{1/2} \sum_{l=\text{even}} \sigma_\rho^-(l)|\Omega\rangle,$$
$$|\rho\rangle_{\text{antifermion}} = \left(\frac{2}{L}\right)^{1/2} \sum_{l=\text{odd}} \sigma_\rho^-(l)|\Omega\rangle \tag{3.9}$$
$$(\rho = 1,2,\ldots,N).$$

One has a $2N$-dimensional degenerate subspace corresponding to the eigenvalue $(2N-1)$. But because of species-number conservation, no mixing between the states will occur.

For states with $n=2$ there are three possible values for B: $B=4$, 3, or 2.

Case 1. The two spins are flipped at the same site $B=2^2=4$. Such states will be interpreted as fermion-fermion (for $l=$even) or antifermion-antifermion (for $l=$odd) bound states:

$$|\rho_1\rho_2\rangle_{FF}=\left(\frac{2}{L}\right)^{1/2}\sum_{l=\text{even}}\sigma^-_{\rho_1}(l)\sigma^-_{\rho_2}(l)|\Omega\rangle\,. \tag{3.10}$$

$(\sigma^-)^2=0$ ensures that $\rho_1\neq\rho_2$, and one has $\frac{1}{2}N(N-1)$ fermion-fermion bound states

$$W_0|\rho_1\rho_2\rangle_{FF}=(4N-4)|\rho_1\rho_2\rangle_{FF}\,,$$

$$Q|\rho_1\rho_2\rangle_{FF}=2|\rho_1\rho_2\rangle_{FF}\,.$$

Similarly one has $\frac{1}{2}N(N-1)$ antifermion-antifermion bound states

$$|\rho_1\rho_2\rangle_{AA}\equiv\left(\frac{2}{L}\right)^{1/2}\sum_{l=\text{odd}}\sigma^-_{\rho_1}(l)\sigma^-_{\rho_2}(l)|\Omega\rangle\,,$$

$$W_0|\rho_1\rho_2\rangle_{AA}=(4N-4)|\rho_1\rho_2\rangle_{AA}\,, \tag{3.11}$$

$$Q|\rho_1\rho_2\rangle_{AA}=-2|\rho_1\rho_2\rangle_{AA}\,.$$

Here, too, species number conservation will ensure that the $N(N-1)\times N(N-1)$ mass matrix remains diagonal to all orders.

Case 2. The two excitations occur at two adjacent sites

$$B=1^2+1^2+1\times1=3\,.$$

These states correspond to fermion-antifermion bound states.

Until now it was not necessary to be careful about phases, since different states were never mixed by the perturbation. However, with the fermion-antifermion bound states, one can have cases where not only $Q=0$ but each individual $Q_\alpha=0$, that is, cases where the two excitations are of the same species. Such states can be mixed by the perturbation V and relative phases become important.

To see what the appropriate phases are, it is necessary to go back to the ϕ-field representation.

Define

$$|l=\text{even},\rho_1\rho_2\rangle_{FA}\equiv(i)^N\{\phi_{\rho_1}(l-1)\,\phi^\dagger_{\rho_2}(l)+\phi_{\rho_1}(l+1)\,\phi^\dagger_{\rho_2}(l)\}|\Omega'\rangle\,. \tag{3.12}$$

Upon performing the Jordan-Wigner transformation, Eq. (2.12), and the transformation (2.15), one has

$$|l=\text{even},\rho_1\rho_2\rangle_{FA}=(i)^{\rho_1+\rho_2}\{\sigma^-_{\rho_1}(l+1)\sigma^-_{\rho_2}(l)-\sigma^-_{\rho_1}(l-1)\sigma^-_{\rho_2}(l)\}|\Omega\rangle\,.$$

Summing again over all even lattice sites and normalizing

$$|\rho_1\rho_2\rangle_{FA}=(i)^{\rho_1+\rho_2}\left(\frac{1}{L}\right)^{1/2}\left\{\sum_{l=\text{even}}\sigma^-_{\rho_2}(l)\sigma^-_{\rho_1}(l+1)-\sum_{l=\text{odd}}\sigma^-_{\rho_1}(l)\sigma^-_{\rho_2}(l+1)\right\}|\Omega\rangle\,. \tag{3.13}$$

There are all together N^2 states of the form (3.13). $N(N-1)$ of them have $\rho_1\neq\rho_2$ and we can omit the phase $(i)^{\rho_1+\rho_2}$. For the N states with $\rho_1=\rho_2$ (3.13) becomes

$$|\rho\rho\rangle_{FA}=(-1)^\rho\left(\frac{1}{L}\right)^{1/2}\sum_{l=1}^{L}(-1)^l\sigma^-_\rho(l)\sigma^-_\rho(l+1)|\Omega\rangle\,. \tag{3.14}$$

These N states will be mixed by the perturbation V.

Case 3. The excitations occur at two nonadjacent sites. $B=2$ for this case. These are states with two free particles.

In the present paper we will consider one- and two-particle states, but it is not hard to see how one would proceed to define bound states with more than two particles.

To organize the perturbation calculations we have found it convenient to label states according to species number $\{Q_\alpha\}$. However, since the lattice Hamiltonian has U(N), and in particular U(1) $\times$SU(N), symmetry, a more natural representation would be one in terms of SU(N) multiplets, with the N one-fermion states of (3.9) corresponding to the fundamental representation of SU(N). This alternative classification of particle states is especially useful in deciding what degeneracies remain to all orders in perturbation theory. For instance, the N^2 fermion-antifermion states of (3.13) consist of an SU(N) singlet and an (N^2-1)-plet since

$$[N]\otimes[\bar{N}]=[N^2-1]\otimes[1]\,. \tag{3.15}$$

In the next section we will see that such additional information provides a good means of checking our calculations.[14]

IV. PERTURBATION CALCULATIONS

In this section we use Rayleigh-Schrödinger perturbation theory to obtain strong-coupling expan-

sions in $x=2/g^2$ for the particle masses. The formulas are again those of Ref. 3:

$$W' = \epsilon_0 + ax^2 + bx^4 + \cdots , \tag{4.1}$$

with

$$a = \left\langle \left| V \frac{1-P}{\epsilon_0 - W_0} V \right| \right\rangle ,$$

$$b = \left\langle \left| V \frac{1-P}{\epsilon_0 - W_0} V \frac{1-P}{\epsilon_0 - W_0} V \frac{1-P}{\epsilon_0 - W_0} V \right| \right\rangle - \left\langle \left| V \frac{1-P}{\epsilon_0 - W_0} V \right| \right\rangle \left\langle \left| V \frac{1-P}{(\epsilon_0 - W_0)^2} V \right| \right\rangle , \tag{4.2}$$

and $W' = W +$ (corrections to the vacuum).

Our task is to evaluate (4.2) for the one- and two-particle states of Sec. III and for the vacuum. To each order one subtracts out the vacuum corrections. The particle energies measured with respect to the shifted vacuum are then identified as the masses of these particles.

Consider first the effects of applying the perturbation V to a given state,

$$V = -(i)^{N+1} \sum_{l=1}^{N} \sum_{\alpha}^{N} \{\sigma_\alpha^+(l)\sigma_\alpha^+(l+1) + (-1)^{N+1}\sigma_\alpha^-(l)\sigma_\alpha^-(l+1)\} \times (-1)^\alpha \sigma_{\alpha+1}^z(l) \cdots \sigma_{\alpha-1}^z(l+1) . \tag{4.3}$$

The term $\sigma_\alpha^{(\mp)}(l)\sigma_\alpha^{(\mp)}(l+1)$ creates (annihilates) two excitations of the same species at two adjacent sites. Since we deal only with states of definite particle number, both creation and annihilation terms will contribute an equal number of times to the matrix elements in (4.2). One can then verify that the factors of $(i)^{N+1}$ and $(-1)^{N+1}$ always conspire to give $+1$ for both even and odd N. The factors of $(-1)^\alpha$ come in pairs for diagonal matrix elements, and for off-diagonal elements they combine with the relative phase $(-1)^\rho$ of Eq. (3.14) giving again just a factor of $+1$. We will still have to consider the phases coming from the σ^z's on a case-by-case basis.

It is convenient to introduce a graphical notation for describing excitations. Let Fig. 3 represent a state with one excitation. This notation does not distinguish between different species. Whenever necessary, such information must be specified separately. Figure 3(b) describes three different states with two excitations. For simplicity, the number "1" will usually be omitted.

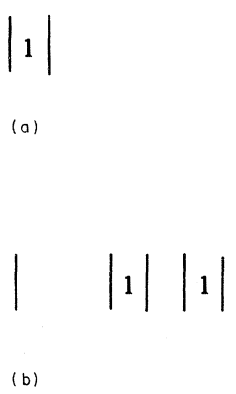

FIG. 3. Diagrammatic notation for excitations: (a) one excitation, (b) two excitations at the same site (for two different species $\alpha_1 \neq \alpha_2$), on nearest-neighbor or on two nonadjacent sites.

By combining the symbols introduced above, one can write down diagrams, describing the history of matrix elements. Going from right to left through a matrix element corresponds to moving from bottom to top of a diagram. Horizontal lines will correspond to vertices, i.e., they will denote creation or annihilation of a pair.

Consider as an example the second-order corrections to the one-fermion state,

$$|\rho\rangle_F = \left(\frac{2}{L}\right)^{1/2} \sum_{l=\text{even}} \sigma_\rho^-(l)|\Omega\rangle . \tag{4.4}$$

The diagrams of Fig. 4 show the four different situations that arise to second order. For each diagram one must calculate the following:

(1) The energy denominator $(\epsilon_0 - W_0)^{-1}$ for the intermediate state, using Eqs. (3.3) and (3.4). Notice that the numbers on the diagrams (after mentally reinserting the 1's) of the horizontal slice corresponding to the intermediate state are just the P_l's of these equations.

(2) The lattice-site-counting factors.

(3) Internal-symmetry-space-counting factors.

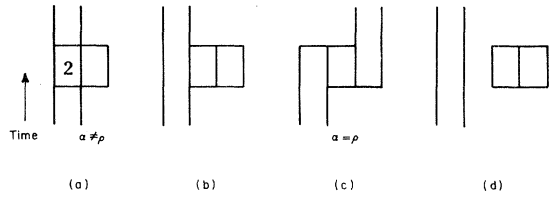

FIG. 4. Second-order diagrams for one-particle states. ρ, α are species labels.

The diagrams (a)–(d) of Fig. 4 give respectively

$$2(N-1)\frac{1}{[(2N-1)-(6N-7)]}=-\frac{2(N-1)}{4N-6}, \quad (4.5a)$$

$$\frac{-2N}{4N-4}, \quad (4.5b)$$

$$\frac{-2}{(4N-4)}, \quad (4.5c)$$

$$-\frac{(L-4)N}{(4N-3)}. \quad (4.5d)$$

The second-order corrections to the vacuum come from diagrams with a single closed box, such as the box of Fig. 4(d). These give

$$\frac{-LN}{(4N-3)}. \quad (4.6)$$

Subtracting (4.6) from (4.5) one is left with the finite, i.e., L-independent, second-order corrections to the one-particle mass:

$$\omega_F^{(2)}=\frac{4N}{4N-3}-\frac{2(N+1)}{4N-4}-\frac{2(N-1)}{4N-6}. \quad (4.7)$$

In the above example the σ^z's in the perturbation (4.3) always gave a factor of $+1$. This is obvious for the diagrams (b)–(d) since excitations never overlap. For diagram (a) one has either $(+1)^2$ or $(-1)^2$ depending on $\alpha \gtrless \rho$.

The calculations of fourth-order corrections to the one-particle mass are somewhat more involved. The three main types of diagrams are shown in Fig. 5. Different time orderings must be considered for all these diagrams. The boxes can also overlap in many ways, giving rise to different energy denominators and counting factors. The contributions coming from Fig. 5 are

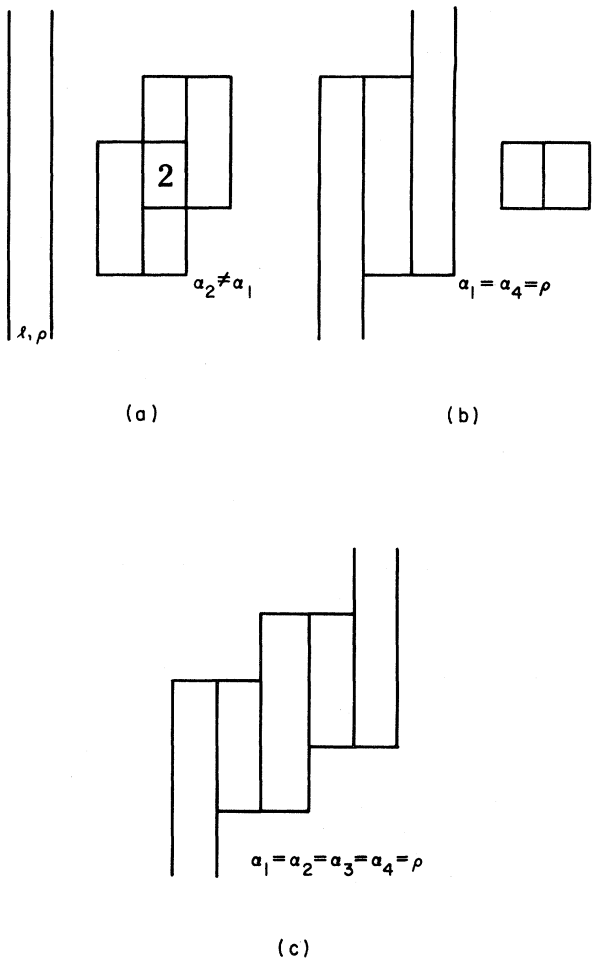

FIG. 5. Fourth-order diagrams for one-particle states.

$$\frac{-1}{(4N-6)^2}\left[\frac{(L-5)2N(N-1)}{4N-3}+\frac{N(N-1)}{4N-5}+\frac{(N-1)^2}{4N-7}+\frac{2(N-1)(N-2)}{4N-8}+\frac{2(N-1)(N-2)}{4N-9}+\frac{2N(N-1)}{8N-11}\right]$$

$$-\frac{1}{(4N-4)^2}\left[\frac{2N(N+1)(L-6)+2(L+1)^2}{4N-3}+\frac{(3N+1)(N+1)}{4N-4}+\frac{3(N^2-1)}{4N-7}+\frac{4(N^2-1)}{8N-11}\right]$$

$$-\frac{1}{(4N-3)^2}\left[\frac{(L-6)(L-7)N^2}{4N-3}+\frac{(L-6)2N(N+1)+N^2+1}{4N-4}+\frac{(L-5)2N(N-1)+N(N-1)}{4N-5}\right.$$

$$\left.+\frac{(L-5)3N(N-1)+N(N-1)}{4N-6}+\frac{2N(N-1)}{8N-11}+\frac{4N^2(L-6)}{8N-7}\right]$$

$$-\frac{2(N^2-1)}{(4N-4)(4N-6)(4N-7)}-\frac{2N(N-1)}{(4N-3)(4N-5)(4N-6)}-\frac{4(N^2-1)}{(4N-4)(4N-6)(8N-11)}$$

$$-\frac{4(N-1)}{(4N-3)(4N-6)(8N-11)}-\frac{4(N^2-1)}{(4N-4)(4N-3)(8N-11)}. \quad (4.8)$$

Fourth-order corrections to the vacuum come from diagrams with two boxes (Fig. 6). These contribute

$$\frac{-LN}{(4N-3)^2}\left[\frac{(L-5)N}{(4N-3)}+\frac{(N-1)}{(4N-6)}+\frac{4N}{(8N-7)}+\frac{2(N-1)}{(4N-5)}\right]. \tag{4.9}$$

One must also calculate the second term in b of Eq. (4.2). For the one-particle states one has

$$-\left\langle\left|V\frac{1-P}{\epsilon_0-W_0}V\right|\right\rangle\left\langle\left|V\frac{1-P}{(\epsilon_0-W_0)^2}V\right|\right\rangle=\left[\frac{(L-4)N}{4N-3}+\frac{2(N+1)}{4N-4}+\frac{2(N-1)}{4N-6}\right]\left[\frac{(L-4)N}{(4N-3)^2}+\frac{2(N+1)}{(4N-4)^2}+\frac{2(N-1)}{(4N-6)^2}\right]. \tag{4.10}$$

The equivalent expression for the vacuum is

$$\frac{L^2N^2}{(4N-3)^3}. \tag{4.11}$$

The desired result, the fourth-order coefficient for the one-particle mass, is

$$\omega_F^{(4)}=[(4.8)+(4.10)]-[(4.9)+(4.11)], \tag{4.12}$$

where the right-hand side lists the appropriate equations. One can verify that Eq. (4.12) is indeed independent of L. The actual values of $\omega_F^{(2)}$ and $\omega_F^{(4)}$ are tabulated in Table II for different N.

Calculations for the fermion-fermion and the antifermion-antifermion bound states are very similar. To fourth order one encounters a new type of diagram, illustrated in Fig. 7. The "X" emphasizes that there is an unexcited site between the two excitations, i.e., one has an intermediate state with two free particles. All other manipulations are identical to those for the one-particle states. The results are also summarized in Table II.

With the fermion-antifermion bound states a few new subtleties appear. The general structure of the W matrix is, in our representation,

$$\begin{vmatrix} C & & & & & & \\ & C & & & & & \\ & & \cdot & & & & \\ & & & \cdot & & & \\ & & & & \cdot & & \\ & & & & C & & \\ & & & & A & D\ \cdots & D \\ & & & & D & A & \\ & & & & \cdot & & \cdot \\ & & & & \cdot & & \\ & & & & \cdot & & \\ & & & & D & & A \end{vmatrix}. \tag{4.13}$$

To lowest order $C=A=4N-3$, $D=0$.

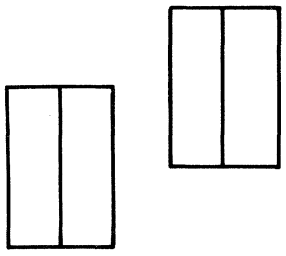

FIG. 6. Fourth-order vacuum corrections.

TABLE II. Strong-coupling expansion coefficients. The values of αN^2 (upper number) and βN^4 (lower number) defined in Eq. (4.21) are tabulated for the following states: F is the one-particle state, FF are the fermion-fermion or antifermion-antifermion states, $FA1$ is the (N^2-1)-plet of fermion-antifermion states, and $FA2$ is the singlet fermion-antifermion state. The first column gives the expansion coefficients for $g\sigma/g\sigma_0$.

N	$g\sigma$	F	FF	$FA1$	$FA2$
4	−0.378 70	−0.463 00	−0.090 58	−0.372 69	−0.423 78
	−0.025 99	−0.043 02	−0.737 51	−0.635 96	−0.801 22
6	−0.326 53	−0.368 83	−0.039 70	−0.246 82	−0.261 22
	0.000 76	0.000 88	−0.730 40	−0.613 19	−0.621 78
8	−0.304 40	−0.332 25	−0.024 88	−0.205 21	−0.212 70
	0.007 49	0.009 09	−0.809 44	−0.707 12	−0.709 02
12	−0.284 44	−0.300 85	−0.014 05	−0.172 47	−0.176 04
	0.011 71	0.013 26	−1.022 83	−0.935 60	−0.935 88
16	−0.275 19	−0.286 78	−0.009 74	−0.158 66	−0.160 95
	0.013 14	0.014 40	−1.257 25	−1.176 97	−1.177 03
20	−0.269 86	−0.278 81	−0.007 44	−0.151 07	−0.152 73
	0.013 83	0.014 87	−1.498 64	−1.422 28	−1.422 28

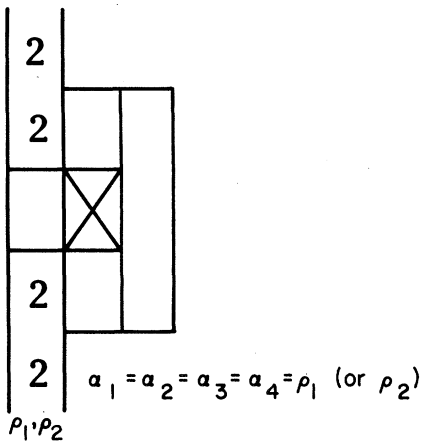

FIG. 7. Example of a diagram with a "hole." These appear for the first time in fourth-order calculations for two-particle states.

To any arbitrary order we know from the remarks at the end of Sec. III that upon diagonalizing (N^2-1) of the eigenvalues must be equal. This implies that

$$C=A-D \tag{4.14}$$

to all orders. We have calculated A, D, and C separately and used (4.14) as a check on our calculations. The eigenvalue for the singlet state is

$$A+(N-1)D\,. \tag{4.15}$$

In evaluating A, D, and C some caution is needed because of the relative minus sign between even and odd sites in Eqs. (3.13) and (3.14). One would expect diagrams where the final and initial states are shifted from each other by an odd number of lattice sites to have a minus sign relative to the corresponding diagram with no shift. This is indeed true for the $\rho_1=\rho_2$ states but not for the cases $\rho_1\neq\rho_2$. In the latter case another factor of (-1) is supplied by the σ^z's in the perturbation.

To give a concrete example, consider the two second-order diagrams of Fig. 8. Diagram (a)

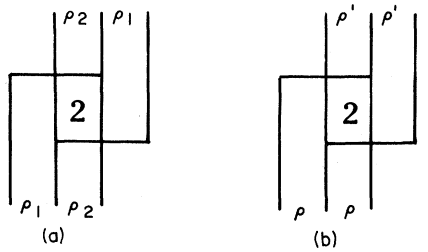

FIG. 8. Second-order diagrams with shifted final states: (a) contribution to C of (4.13), (b) contribution to D.

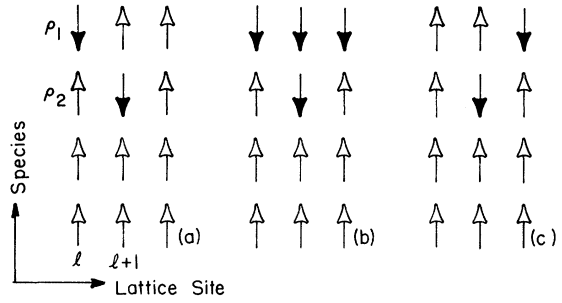

FIG. 9. Detailed analysis of Fig. 8(a): (a) initial configuration, (b) intermediate configuration, (c) final configuration.

contributes to the matrix elements C of (4.13) and diagram (b) to the off-diagonal elements D. Figure 9 analyzes Fig. 8 in more detail, showing from left to right the initial, the intermediate, and the final states, for $N=4$. One sees that in going to the final state the operator $\sigma_1^z(l+1)\sigma_2^z(l+1)\sigma_3^z(l+1)$ gives a factor of (-1). A similar analysis of Fig. 8(b), depicted in Fig. 10, shows no such additional factors of (-1) arising.[15] Even to fourth order the relative minus sign between even and odd final states will always be canceled for the $\rho_1\neq\rho_2$ states.

We have also calculated $g\sigma\equiv-g^2\langle\bar{\psi}_c\psi_c\rangle_{\rm vac}$ to fourth order. In our representation $g\sigma$ becomes[16]

$$g\sigma=-\frac{g^2}{La}\left\langle-\tfrac{1}{2}\sum_{l}^{L}\sum_{\alpha}^{N}\sigma_\alpha^z(l)\right\rangle_{\rm vac}\,. \tag{4.16}$$

To obtain the vacuum expectation value in (4.16), consider the following operator:

$$U\equiv U_0+xV\equiv W_0-\frac{\lambda}{2}\sum_{l}^{L}\sum_{\alpha}^{N}\sigma_\alpha^z(l)+xV\,. \tag{4.17}$$

Then

$$\left\langle-\tfrac{1}{2}\sum_{l}^{L}\sum_{\alpha}^{N}\sigma_\alpha^z(l)\right\rangle_{\rm vac}=\frac{\partial}{\partial\lambda}\langle U\rangle_{\rm vac}\Big|_{\lambda=0}\,, \tag{4.18}$$

$$g\sigma=-\frac{g^2}{La}\frac{\partial}{\partial\lambda}\langle U\rangle_{\rm vac}\Big|_{\lambda=0}\,. \tag{4.19}$$

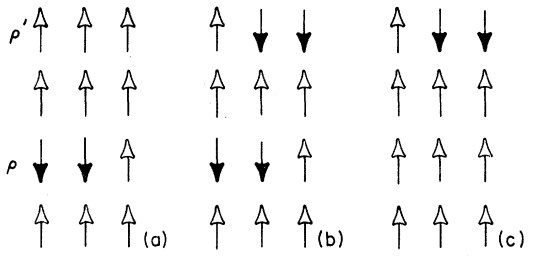

FIG. 10. Same as Fig. 9 for an analysis of Fig. 8(b).

$\langle U\rangle_{\rm vac}$ can be evaluated order by order in x^2:

$$\langle U\rangle_{\rm vac} = U^{(0)} + U^{(2)}x^2 + U^{(4)}x^4 + \cdots ,$$

$$U^{(0)} = -\frac{\lambda}{2} LN ,$$

$$U^{(2)} = -\frac{LN}{(4N+2\lambda-3)} ,$$

$$U^{(4)} = \frac{LN}{(4N+2\lambda-3)^2}\left[\frac{5N}{(4N+2\lambda-3)} - \frac{4N}{(8N+4\lambda-7)} - \frac{2(N-1)}{(4N+2\lambda-5)} - \frac{(N-1)}{(4N+2\lambda-6)}\right] , \tag{4.20}$$

$$g\sigma = (g\sigma_0)\left[1 - \frac{2}{LN}\left(\frac{\partial}{\partial\lambda}U^{(2)}\right)_{\lambda=0}x^2 - \frac{2}{LN}\left(\frac{\partial}{\partial\lambda}U^{(4)}\right)_{\lambda=0}x^4\right] ,$$

with

$$g\sigma_0 = g^2N/2a .$$

All the results for strong-coupling expansion coefficients are summarized in Table II. In analogy with Eq. (4.20) we have factored out the zeroth-order values in presenting the coefficients and the following notation has been adopted:

$$W\ (\text{or } g\sigma) = \omega^{(0)}(1 + \alpha x^2 + \beta x^4) \tag{4.21}$$

and F is the one-particle state, FF are the fermion-fermion or antifermion-antifermion bound states, and $FA1$ is the (N^2-1)-plet of fermion-antifermion bound states, and $FA2$ is the singlet fermion-antifermion bound state. In order to avoid very small numbers, we have tabulated the values for αN^2 and βN^4. In effect we are using $2/g^2N$ as the expansion parameter at this point.

V. THE CONTINUUM LIMIT

In the preceding three sections we set up the SU(N) Thirring model on a lattice and identified the one-particle states and the two-particle bound states. Then we performed fourth-order strong-coupling calculations for the masses of these states. These results were obtained at some fixed lattice spacing a and for a coupling constant $g^2(a)$ defined to be large. A comparison with continuum theories makes sense only if we are first able to extend our results to the continuum. In the Introduction we explained how this can be accomplished. Following the prescription outlined and motivated there, we will write Padé approximants for the perturbation series of Sec. IV and then go to the continuum limit by letting $g^2 \to 0$ ($x \to \infty$). We will see that in some cases, higher-order calculations are needed to obtain meaningful continuum limits. However, in many cases surprisingly good results are found already at fourth order.

Consider the [1,1] Padé approximants for particle masses measured in units of $g\sigma$:

$$\frac{M}{g\sigma} = \frac{(M/g\sigma)_0 + px^2}{1+qx^2} . \tag{5.1}$$

The coefficients "p" and "q" have been tabulated in Table III. For the two-particle states both p and q are positive so the continuum limit, $x^2 \to \infty$, can be taken in a singularity-free fashion,

$$\left(\frac{M}{g\sigma}\right)_{\rm continuum} = \frac{p}{q} . \tag{5.2}$$

These continuum limits are shown in Table III, together with the zeroth-order strong-coupling result $(M/g\sigma)_0$, and the DHN values,

$$\left(\frac{M}{g\sigma}\right)_{\rm DHN} = \frac{2N}{\pi}\sin\left(\frac{\pi}{2N}n\right) \tag{5.3}$$

($n = 2$ in the present case).

One sees that the continuum values are in *better*

TABLE III. [1,1] Padé approximants and continuum limit of $M/g\sigma$. The quantities p and q are defined in Eq. (5.1), the [1,1] Padé approximant for $M/g\sigma$. F, FF, $FA1$, and $FA2$ are as defined for Table II. The third to fifth columns show respectively the strong-coupling lattice results, the continuum limit, and the DHN values.

N		p	q	$\left(\frac{M}{g\sigma}\right)_0$	p/q	$\left(\frac{M}{g\sigma}\right)_{\rm DHN}$
4	F	−0.036 37	−0.036 30	0.875		0.974
	FF	0.223 03	0.130 68	1.500		1.801
	$FA1$	10.268 16	6.318 49	1.625		
	$FA2$	−1.789 48	−1.098 40	1.625		
6	F	−0.009 32	−0.008 99	0.917		0.989
	FF	0.116 18	0.061 74	1.667	1.882	1.910
	$FA1$	0.362 41	0.204 88	1.750	1.769	
	$FA2$	0.450 69	0.255 72	1.750	1.762	
8	F	−0.004 02	−0.003 86	0.938		0.996
	FF	0.079 23	0.040 91	1.750	1.937	1.949
	$FA1$	0.198 23	0.107 82	1.813	1.839	
	$FA2$	0.215 27	0.117 33	1.813	1.835	
12	F	−0.001 37	−0.001 32	0.958		0.997
	FF	0.048 53	0.024 59	1.833	1.974	1.977
	$FA1$	0.107 91	0.056 78	1.875	1.900	
	$FA2$	0.111 52	0.058 73	1.875	1.899	
16	F	−0.000 67	−0.000 65	0.969		0.998
	FF	0.034 98	0.017 62	1.875	1.985	1.987
	$FA1$	0.074 87	0.038 82	1.906	1.929	
	$FA2$	0.076 37	0.039 62	1.906	1.928	
20	F	−0.000 40	−0.000 38	0.975		0.999
	FF	0.027 34	0.013 73	1.900	1.991	1.992
	$FA1$	0.057 45	0.029 55	1.925	1.944	
	$FA2$	0.058 27	0.029 98	1.925	1.944	

agreement with DHN than the strong-coupling results. Figure 11 shows a plot of (5.2) and (5.3) as a function of N. In Fig. 12 we have plotted the [1.1] Padé approximant, Eq. (5.1), for $N=6$, 12, and 20.

However, when we apply Eq. (5.1) to the single fermion state a curious problem arises. Notice from Table III that then $q<0$ and $p<0$ while $|p|>|q|$. Therefore $M/g\sigma$ becomes negative for a finite, but large value of x and our [1, 1] Padé approximants will have ceased to be meaningful. Experience with extrapolation methods suggests that this may not be a serious problem. Note that we are writing Padé approximants for the ratios of two very similar Taylor series (see Table II). Very small differences in the Taylor series are therefore controlling the qualitative character of the [1, 1] Padé approximants. Under these circumstances low-order Padé approximants may not be reliable but higher-order approximants should resolve this difficulty.

We have also calculated [1, 1] Padé approximants for the ratios of bound-state masses to the fermion mass

$$\frac{M_{FF}\ (\text{or}\ M_{FA})}{M_F}=\frac{(M_{FF,A}/M_F)_0+p'x^2}{1+q'x^2} \tag{5.4}$$

Table IV summarizes the values for p' and q', and Fig. 13 shows plots of Eq. (5.4). The fermion-antifermion states, as shown in Fig. 11, are again in good agreement with the DHN values but, as shown in Fig. 13, the FF states seem to become barely unbound in the continuum limit. The main difference in our calculations between the FF and the FA states lies in the second-order correction $\omega^{(2)}$, or αN^2 of Table II. This difference arises from the way in which we chose to set up the theory on a lattice, i.e., one has both excitations

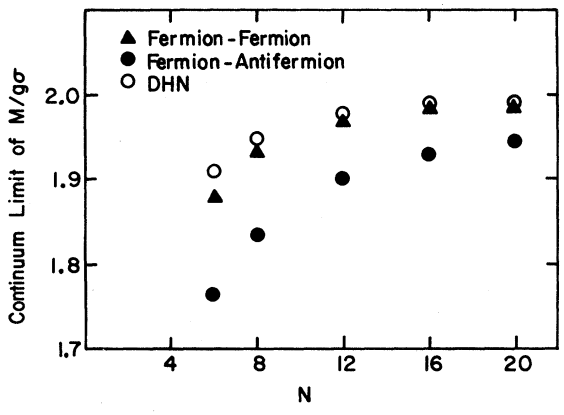

FIG. 11. Continuum limit of particle masses, measured in units of $g\sigma$, and comparison with DHN.

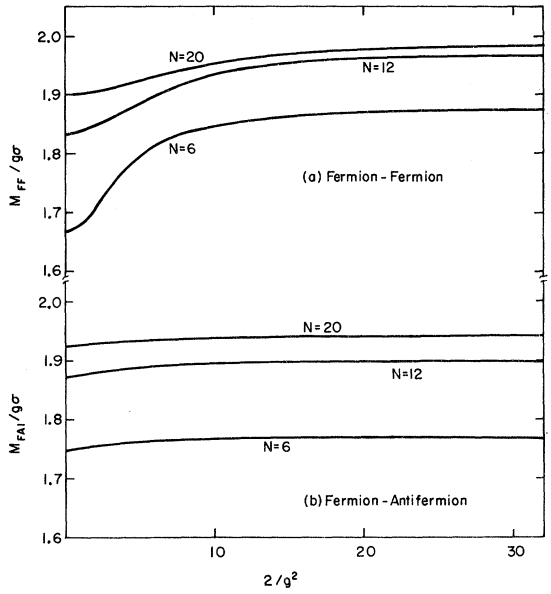

FIG. 12. [1, 1] Pade approximants for $M/g\sigma$ [Eq. (5.1)]: (a) fermion-fermion bound states, (b) fermion-antifermion bound states.

TABLE IV. [1, 1] Padé approximants and continuum limit of mass ratios. Same comments apply here as for Table III except that they refer to Eq. (5.4), the [1, 1] Padé approximant for M/M_F.

N		p'	q'	$\left(\frac{M_2}{M_F}\right)_0$	p'/q'	$\left(\frac{M_2}{M_F}\right)_{\text{DHN}}$
4	FF	0.190 09	0.087 61	1.714	2.170	1.848
	$FA1$	0.718 77	0.381 38	1.857	1.885	
	$FA2$	2.194 57	1.179 24	1.857	1.861	
6	FF	0.110 21	0.051 47	1.818	2.141	1.932
	$FA1$	0.253 80	0.129 56	1.909	1.959	
	$FA2$	0.293 00	0.150 49	1.909	1.947	
8	FF	0.076 95	0.036 42	1.867	2.113	1.962
	$FA1$	0.164 12	0.082 90	1.933	1.980	
	$FA2$	0.175 04	0.088 67	1.933	1.974	
12	FF	0.047 81	0.023 00	1.913	2.079	1.983
	$FA1$	0.098 08	0.049 24	1.957	1.992	
	$FA2$	0.100 93	0.050 72	1.957	1.990	
16	FF	0.034 63	0.016 81	1.935	2.060	1.990
	$FA1$	0.070 26	0.035 20	1.968	1.996	
	$FA2$	0.071 54	0.035 86	1.968	1.995	
20	FF	0.027 14	0.013 25	1.949	2.048	1.994
	$FA1$	0.054 79	0.027 43	1.974	1.997	
	$FA2$	0.055 51	0.027 80	1.974	1.997	

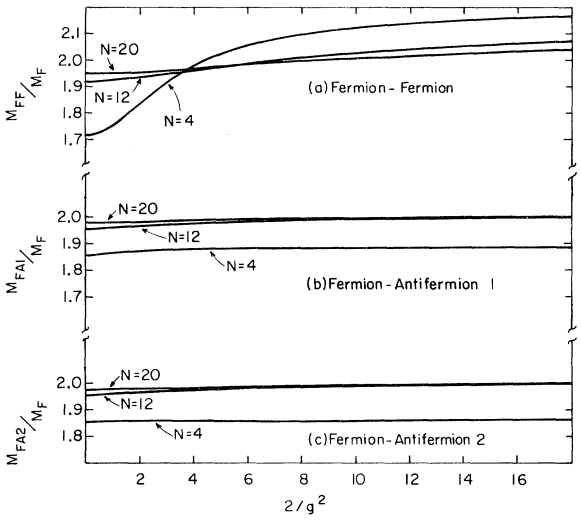

FIG. 13. [1,1] Pade approximants for ratios of two-particle to one-particle states [Eq. (5.4)].

at the same site for the FF states but at adjacent sites for the FA states. We believe that by going to higher orders the continuum limit will become independent of such specifics of the lattice theory. The FF and FA states may then become degenerate and the FF states remain bound. In higher orders the two different procedures, Eqs. (5.1) and (5.4), for taking the continuum limit should become identical.

An indication that the apparent unboundedness of the FF states to fourth order may be deceptive is found by comparing these states to spatially antisymmetric fermion-antifermion states, i.e., to states obtained by changing the relative sign between the two terms in Eq. (3.12). We expect most of these latter states to become unbound in the continuum limit since, except for the SU(N) singlet, a nonrelativistic δ-function potential picture is applicable and only spatially symmetric states will be bound.[6] Upon calculating $M_{(\text{two particle})}/M_F$ for spatially antisymmetric states, we find that the (N^2-1)-plet states do indeed become unbound in the continuum limit, to a much more unambiguous degree than the FF states [see Fig. 14 and note the different vertical scales on (a) and (b)]. The SU(N) singlet state remains below threshold and this leads us to conjecture that it corresponds to the O($2N$) singlet "σ bound state" of DHN. As these authors point out, annihilation graphs become dominant for the singlet state, and these give rise to an attractive interaction.

Finally, we want to make a consistency check on the following:

(1) our assumption that the gap equation is describing the behavior of $2aM_F$, and also of $g\sigma$, not

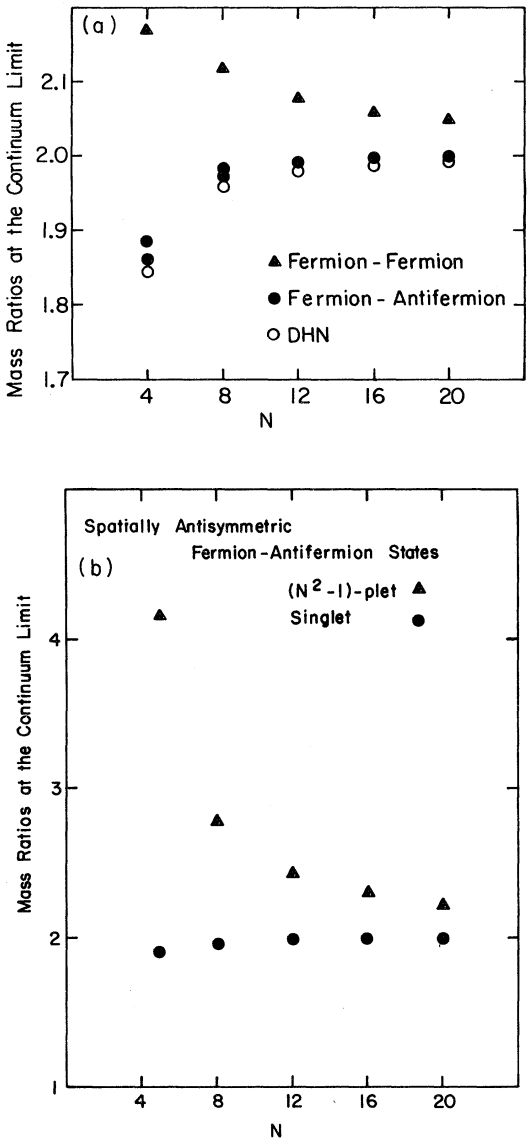

FIG. 14. Mass ratios at the continuum limit and comparison with DHN: (a) two-particle states defined in Sec. III, (b) fermion-antifermion states with spatially antisymmetric wave functions [obtained by changing the sign in Eq. (3.12)]. Note the different vertical scales in (a) and (b).

only at the two extremes $g^2(a) \gg 1$ and $g^2(a) \ll 1$, but also over the whole range of $g^2(a)$ (recall that this assumption was a crucial factor in motivating our limiting procedure), and

(2) our claim that Padé approximants provide a reliable means of extending the region of validity of strong-coupling expansions, and in particular of taking the continuum limit.

To do this we can compare $2a\Delta$ as calculated

using the gap equation with $2aM_F$ and $g\sigma$ as calculated using strong-coupling perturbation theory. If our method of taking the continuum limit is good, these quantities should agree over a wide range of x^2. We are interested to find the value of $g(a)$, where a discrepancy is first appreciable. If it turns out that this value of $g(a)$ is small, then our extrapolation procedure from $g^2=\infty$ to the continuum limit is probably sound and our success in calculating parts of the mass spectrum of this theory becomes understandable.

To do this most critically we have looked at the deviations from linear dependency on g^2 of the three quantities $2aM_F$, $g\sigma$, and $2a\Delta$. In the Appendix we derive the gap equation

$$\frac{1}{g^2(a)}=\frac{(2N-1)}{2\pi a\Delta}(1+m)^{-1/2}K\left(\frac{m}{1+m}\right), \tag{5.5}$$

with $m=1/a^2\Delta^2$, $K(x)$ = complete elliptic integral of the first kind.

In the strong-coupling (large $a\Delta$) limit (5.5) leads to

$$(2a\Delta)_0=\frac{(2N-1)}{2}g^2. \tag{5.6}$$

Equation (5.5) can be inverted (graphically) so that it is possible to plot

$$\frac{2a\Delta}{(2a\Delta)_0}=\frac{2a\Delta}{(2N-1)g^2/2}, \tag{5.7}$$

where the numerator is a function of $2/g^2$.

For $2aM_F$ and $g\sigma$, on the other hand, one has, using the notation of Eq. (4.21),

$$\frac{2aM_F}{(2aM_F)_0}=\frac{W}{\omega^{(0)}}=1+\alpha x^2+\beta x^4, \tag{5.8}$$

$$\frac{g\sigma}{(g\sigma)_0}=1+\alpha_\sigma x^2+\beta_\sigma x^4. \tag{5.9}$$

In Fig. 15 we have plotted (5.7) and the [1, 1] Padé approximants for Eqs. (5.8) and (5.9). The Padé approximants definitely show better agreement with (5.7) than the zeroth-order strong-coupling result. They are able to retrace the gap equation curve to $g^2/2\sim 1/N$. So, for SU(6), say, the diagonal Padé approximant method is an accurate extrapolation method from $g^2=\infty$ to $g^2/2\approx\frac{1}{6}$.

VI. DISCUSSION

Following the application of lattice Hamiltonian methods to the Schwinger model,[3] the present paper has taken us through another exercise in employing a spatial lattice as a computational tool to obtain the spectrum of a continuum field theory. The main purpose in performing these calculations in simple one-dimensional theories is to gain experience and a better understanding of the nature of our approximation scheme.

In the present paper we obtained [1,1] Padé approximants for M/M_F and $M/g\sigma$ and for the one-particle mass (in units of $1/2a$). Where it was possible to take the continuum limit, the values obtaind for $(M/M_F)_{\text{continuum}}$ and $(M/g\sigma)_{\text{continuum}}$ seem to indicate that fourth-order results can already be quite reliable. But one will have to go to higher orders to be able to claim more definitely that the sequence of diagonal Padé approximants is converging toward the correct continuum value. We also hope that higher-order calculations will remedy some of the difficulties we are having at the present level with $M_F/g\sigma$, and that they will show indications of the full $O(2N)$ symmetry of the continuum theory and bring the FF and FA states closer together.

Finally, it will be interesting to see whether the Padé approximants for $2aM_F$ and $g\sigma$ themselves will retrace the gap equation curve further into the weak-coupling domain. Since Eq. (A21) states that the gap, $a\Delta$, has an essential singularity[17] at $x=\infty$, experience with Padé approximants suggests

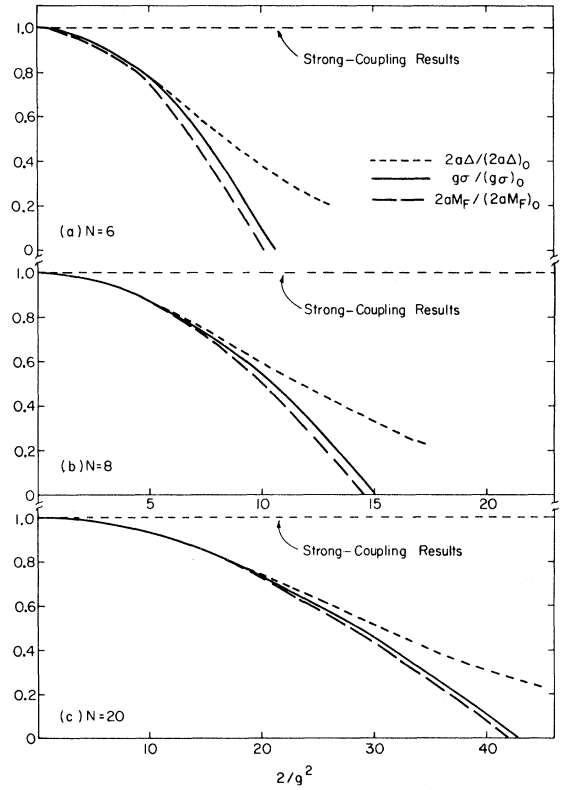

FIG. 15. Comparison of $2a\Delta/(2a\Delta)_0$, $2aM_F/(2aM_F)_0$, and $g\sigma/(g\sigma)_0$ as one approaches the continuum limit ($g^2\to 0$). $2a\Delta/(2a\Delta)_0$ is obtained from the gap equation. The curves for $2aM_F/(2aM_F)_0$ and $g\sigma/(g\sigma)_0$ correspond to the [1, 1] Padé approximants of strong-coupling expansions.

that the sequence of $[N,N]$ approximants will not converge uniformly to the continuum limit. We expect instead that each $[N,N]$ approximant will be reliable from $g^2=\infty$ to some particular value of g^2. As higher-order calculations are done, so that $[N+M,N+M]$ approximants are made, the range in g^2 over which the extrapolation method works should (we hope) become larger and larger. We plan to investigate this speculation by calculating higher orders using computer methods. We also suspect that sequences of diagonal Padé approximants *will* converge uniformly for *dimensionless* mass ratios and matrix elements. Overall essential singularities cancel in such ratios which could, therefore, be relatively simple functions of complex x. Higher-order calculations in simpler, superrenormalizable models[3] did in fact suggest uniform and quick convergence for dimensionless quantities.

There are still many open questions even in this one-dimensional model, but work is in progress to investigate some of them by going to eighth order in strong-coupling perturbation. We are also looking at states with more than two excitations, and we hope to be able to establish a one-to-one correspondence between the DHN spectrum and bound states obtained by lattice Hamiltonian methods.

ACKNOWLEDGMENTS

One of us (J.S.) would like to thank John Kogut for suggesting this topic and for giving generously of his time for many useful discussions. His help in preparing this manuscript is also gratefully acknowledged. S. Elitzur thanks T. Banks, J. Kogut and L. Susskind for helpful discussions.

APPENDIX: THE GAP EQUATION

In this appendix we derive a generalization of the gap equation (5.5) appropriate for any SU(N). The large-N result is identical to that obtained by Zee.[7]

We shall use the following momentum-space representation for the fermion fields ϕ:

$$\phi_\alpha(l=\text{even})=\left(\frac{2}{L}\right)^{1/2}\sum_p (\text{sgn}p)a_\alpha(p)e^{ipla},$$
$$\phi_\alpha(l=\text{odd})=\left(\frac{2}{L}\right)^{1/2}\sum_p b^\dagger_\alpha(p)e^{-ipla}, \tag{A1}$$

where

$$p=\frac{2\pi}{aL}n,$$
$$n=\pm 1,\pm 2,\ldots,\pm\frac{L}{4}.$$

Equation (A1) corresponds in the continuum limit to a representation appropriate for describing very massive free fermions

$$\psi^c_\alpha(z)=\int\frac{dp}{2\pi}\left[\begin{pmatrix}\text{sgn}p\\0\end{pmatrix}a_\alpha(p)e^{ipz}+\begin{pmatrix}0\\1\end{pmatrix}b^\dagger_\alpha(p)e^{-ipz}\right]. \tag{A2}$$

Substituting (A1) into the expression (2.19) for the lattice Hamiltonian, one has

$$H_{\text{kin}}=\frac{1}{a}\sum_p\sum_{\alpha=1}^N(\text{sgn}p)\sin pa\{a^\dagger_\alpha(p)b^\dagger_\alpha(-p)+b_\alpha(-p)a_\alpha(p)\},$$
$$H_{\text{pot}}=-\frac{g^2}{2a}\frac{1}{L}\sum_{p,k,q}\sum_{\alpha,\beta}^N\{(\text{sgn}p)(\text{sgn}(p-q))(\text{sgn}k)(\text{sgn}(k+q))(a^\dagger_\alpha(p)a_\alpha(p-q))(a^\dagger_\beta(k)a_\beta(k+q))$$
$$+(b_\alpha(p)b^\dagger_\alpha(p-q))(b_\beta(k)b^\dagger_\beta(k+q))$$
$$-2(\text{sgn}k)(\text{sgn}(k-q))\cos qa(a^\dagger_\alpha(k)a_\alpha(k-q))(b_\beta(p)b^\dagger_\beta(p-q))\}. \tag{A3}$$

We shall now perform a Bogoliubov transformation[18] and minimize the ground-state energy with respect to the Bogoliubov angle θ_p. Let

$$U_p=\cos\theta_p,\quad V_p=\sin\theta_p. \tag{A4}$$

The transformation is

$$a_\alpha(p)=U_p c_\alpha(p)-V_p d^\dagger_\alpha(-p),$$
$$b_\alpha(-p)=U_p d_\alpha(-p)+V_p c^\dagger_\alpha(p). \tag{A5}$$

In (A5) θ_p is independent of the species label α.

We next normal-order the Hamiltonian with respect to the new ground state $|\Omega\rangle$ defined by

$$c_\alpha(p)|\Omega\rangle=d_\alpha(p)|\Omega\rangle=0. \tag{A6}$$

The relevant contractions (denoted by corresponding sets of superscripts on the operators being contract-

ed) are

$$a_\alpha^{\dagger\cdot}(p)a_{\alpha'}^{\cdot}(p')=b_\alpha^{\dagger\cdot}(-p)b_{\alpha'}^{\cdot}(-p')=V_p^2\delta_{\alpha\alpha'}\delta_{pp'},$$

$$a_\alpha^{\dagger\cdot}(p)b_{\alpha'}^{\dagger\cdot}(-p')=b_\alpha^{\cdot}(-p)a_{\alpha'}^{\cdot}(p')=-U_pV_p\delta_{\alpha\alpha'}\delta_{pp'}, \tag{A7}$$

$$b^{\dagger\cdot}a^{\cdot}=a^{\dagger\cdot}b^{\cdot}=0.$$

The resulting expression for H is

$$H=:H:+H_2+H_1,$$

where

$$H_2=\frac{g^2}{a}\frac{1}{L}\sum_{k,p}\sum_{\alpha}^{N}\{(\mathrm{sgn}k)(\mathrm{sgn}p)[\cos(k-p)a]U_pV_p[:b_\alpha(-k)a_\alpha(k):+a_\alpha^\dagger(k)b_\alpha^\dagger(-k)]$$
$$-(2N-1)(V_p^2-\tfrac{1}{2})[:a_\alpha^\dagger(k)a_\alpha(k):+:b_\alpha^\dagger(k)b_\alpha(k):]\}$$
$$+\frac{1}{a}\sum_p\sum_\alpha^N(\mathrm{sgn}p)\sin pa[:b_\alpha(-p)a_\alpha(p):+:a_\alpha^\dagger(p)b_\alpha^\dagger(-p):] \tag{A8}$$

and

$$H_1=-\frac{g^2}{a}\frac{1}{L}\sum_{k,p}\{N(2N-1)V_k^2(V_k^2-1)+N(\mathrm{sgn}k)(\mathrm{sgn}p)[\cos(k-p)a]U_kV_kU_pV_p\}$$
$$-\frac{2N}{a}\sum_p(\mathrm{sgn}p)(\sin pa)U_pV_p. \tag{A9}$$

One can now minimize $\langle\Omega|H|\Omega\rangle=H_1$ with respect to U and V ($U^2+V^2=1$), or alternatively require that H_2 be diagonal in the operators $c_\alpha(p)$ and $d_\alpha(p)$.[18] Taking the latter approach, define

$$\Delta_p\equiv(2N-1)\frac{g^2}{aL}\sum_k(\tfrac{1}{2}-V_k^2)\equiv\Delta(\text{independent of }p),$$
$$\xi_p\equiv\frac{(\mathrm{sgn}p)}{a}\left\{\sin pa+\frac{g^2}{L}\sum_k(\mathrm{sgn}k)U_kV_k[\cos(k-p)a]\right\} \tag{A10}$$

Then

$$H_2=\sum_p\sum_\alpha^N\{\xi_p[:a_\alpha^\dagger(p)b_\alpha^\dagger(-p):+:b_\alpha(-p)a_\alpha(p):]+\Delta_p[:b_\alpha^\dagger(p)b_\alpha(p):+:a_\alpha^\dagger(p)a_\alpha(p):]\}$$
$$=\sum_p\sum_\alpha\{\xi_p[\cos2\theta_p(c_\alpha^\dagger(p)d_\alpha^\dagger(-p)-c_\alpha(p)d_\alpha(-p))+\sin2\theta_p(d_\alpha^\dagger(-p)d_\alpha(-p)+c_\alpha^\dagger(p)c_\alpha(p))]$$
$$+\Delta_p[\cos2\theta_p(d_\alpha^\dagger(-p)d_\alpha(-p)+c_\alpha^\dagger(p)c_\alpha(p))-\sin2\theta_p(c_\alpha^\dagger(p)d_\alpha^\dagger(-p)-c_\alpha(p)d_\alpha(-p))]\}. \tag{A11}$$

The requirement that the off-diagonal terms in (A11) cancel leads to

$$\tan2\theta_p=\xi_p/\Delta. \tag{A12}$$

So one has

$$\sin2\theta_p=\frac{\xi_p}{(\xi_p^2+\Delta^2)^{1/2}},$$
$$\cos2\theta_p=\frac{\Delta}{(\xi_p^2+\Delta^2)^{1/2}}, \tag{A13}$$
$$\tfrac{1}{2}-\sin^2\theta_p=\frac{1}{2}\frac{\Delta}{(\xi_p^2+\Delta^2)^{1/2}}.$$

Inserting (A13) back into our definitions for Δ and ξ_p one finds the following set of coupled consistency equations:

$$\Delta=(2N-1)\frac{g^2}{aL}\sum_k\frac{1}{2}\frac{\Delta}{(\xi_k^2+\Delta^2)^{1/2}}, \tag{A14}$$

$$a\xi_p=(\mathrm{sgn}p)\sin pa\left\{1+\frac{g^2}{L}\sum_{k>0}\frac{\xi_k}{(\xi_k^2+\Delta^2)^{1/2}}\sin ka\right\}. \tag{A15}$$

In deriving (A15) we have made the further restriction that $\theta_p=\theta_{-p}$. Equation (A14) can be written as

$$\frac{1}{g^2}=\frac{(2N-1)}{L}\sum_{k>0}\frac{1}{(a^2\xi_k^2+a^2\Delta^2)^{1/2}}. \tag{A16}$$

Equation (A16) can be interpreted as a (mean-field) renormalization-group equation for the running coupling constant $g^2(a)$. Note that Eq. (A11) implies that Δ is the mass of the fermion excitations which diagonalize H in the mean-field approximation. Therefore, Eq. (A16) indicates how g must be varied as a function of a in order that Δ be a fixed, physical quantity.

Equations (A15) and (A16) were solved iteratively by numerical methods beginning with

$$a\xi_p^{(0)} = \sin pa \tag{A17}$$

and using

$$\frac{1}{(g^{(n+1)})^2} = \frac{2N-1}{a\Delta}\frac{1}{L}\sum_{k>0}\frac{1}{\{1+[1/(a\Delta)^2](a\xi_k^{(n)})^2\}^{1/2}}, \tag{A18}$$

$$a\xi_p^{(n+1)} = \sin pa\left\{1+\frac{(g^{(n+1)})^2}{a\Delta}\frac{1}{L}\times\sum_{k>0}\frac{(\sin ka)a\xi_k^{(n)}}{\{1+[1/(a\Delta)^2](a\xi_k^{(n)})^2\}^{1/2}}\right\}.$$

In evaluating the summation over modes, the large-L limit was taken and

$$\frac{1}{L}\sum_{k>0}\to\frac{1}{2\pi}\int_0^{\pi/2}d\theta$$

with

$$\theta = ka = \frac{2\pi}{L}n.$$

As long as $N\gtrsim 4$ no significant changes in the values for g^2 were produced by these iterations, for any fixed but arbitrary $a\Delta$. So henceforth we will use the approximation (A17) and[19]

$$\frac{1}{g^2} = \frac{(2N-1)}{L}\sum_{k>0}\frac{1}{[a^2\Delta^2+(\sin ka)^2]^{1/2}}. \tag{A19}$$

Consider first the asymptotic behavior of (A19):

1. $a\Delta \gg 1$ (large spatial cutoff)

$$\frac{1}{g^2}\approx\frac{(2N-1)}{L}\frac{1}{a\Delta}\sum_{k>0}=\frac{(2N-1)}{4a\Delta}$$

or

$$\Delta = \frac{g^2}{4a}(2N-1). \tag{A20}$$

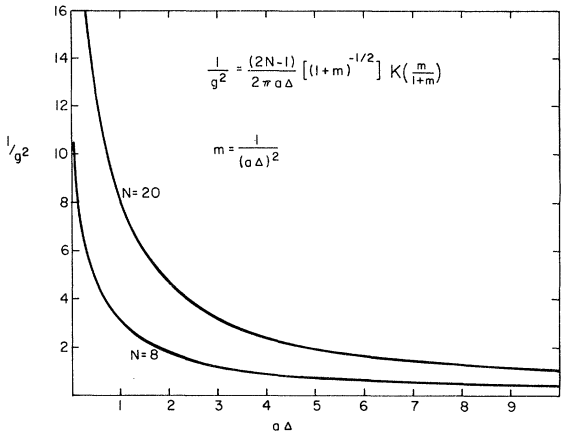

FIG. 16. Plot of the gap equation (A22).

Note that (A20) is exactly the energy of the one-particle state calculated in zeroth-order strong-coupling approximation [see Eq. (3.8) of text and recall that $H_0 = (g^2/4a)W_0$].

2. $a\Delta \ll 1$ (small spatial cutoff)

$$\frac{1}{g^2} = \frac{(2N-1)}{2\pi}\int_0^{\pi/2}\frac{d\theta}{[\sin^2\theta+(a\Delta)^2]^{1/2}} \underset{a\Delta\to 0}{\sim}\frac{(2N-1)}{2\pi}(-\ln a\Delta)$$

or

$$a\Delta \propto \exp[-2\pi/(2N-1)g^2]. \tag{A21}$$

For large N we have $\Delta\propto\exp(-\pi/Ng^2)$, which agrees with the one-loop renormalization-group calculation of Gross and Neveu.[5]

In general (A19) can be written in terms of a complete elliptical integral of the first kind $K(x)$,[20]

$$\frac{1}{g^2} = \frac{(2N-1)}{a\Delta}\frac{1}{L}\sum_{k>0}\frac{1}{[1+(1/a^2\Delta^2)(\sin ka)^2]^{1/2}} \to\frac{(2N-1)}{2\pi a\Delta}\int_0^{\pi/2}(1+m\sin^2\theta)^{-1/2}d\theta = \frac{(2N-1)}{2\pi a\Delta}(1+m)^{-1/2}K\left(\frac{m}{1+m}\right), \tag{A22}$$

where $m = 1/(a\Delta)^2$. Equation (A22) is shown in Fig. 16 for $N=8$ and $N=20$.

*Work supported in part by the National Science Foundation.

†Work supported in part by the Israel Commission for Basic Research.

[1]Lattice gauge theory was invented by K. G. Wilson, Phys. Rev. D 10, 2445 (1974), and A. M. Polyakov (unpublished).

[2]The Hamiltonian formalism is discussed in J. Kogut and L. Susskind, Phys. Rev. D 11, 395 (1975).

[3]For a recent application of the lattice Hamiltonian methods to the Schwinger model, see T. Banks, L. Susskind, and J. Kogut, Phys. Rev. D 13, 1043 (1976); A. Carroll, J. Kogut, D. K. Sinclair, and L. Susskind, *ibid.* 13, 2270 (1976); 14, 1729(E) (1976).

[4]The Abelian model was introduced by W. Thirring, Ann. Phys. (N.Y.) 3, 91 (1958). It was solved by K. Johnson, Nuovo Cimento 20, 773 (1961).
[5]D. J. Gross and A. Neveu, Phys. Rev. D 10, 3235 (1974).
[6]R. F. Dashen, B. Hasslacher, and A. Neveu, Phys. Rev. D 12, 2443 (1975).
[7]A. Zee, Phys. Rev. D 12, 3251 (1975).
[8]Y. Nambu and G. Jona-Lasinio, Phys. Rev. 122, 345 (1961).
[9]George A. Baker, Jr., *Essentials of Padé Approximants* (Academic, New York, 1975). A particularly relevant discussion appears in the Appendix to J. Kogut, D. K. Sinclair, and L. Susskind, Cornell Report No. CLNS-336, 1976 (unpublished) [Nucl. Phys. B (to be published)].
[10]S. Coleman and E. Weinberg, Phys. Rev. D 7, 1888 (1973).
[11]Y. Aharonov, A. Casher, and L. Susskind, Phys. Rev. D 5, 988 (1972).
[12]P. Jordan and E. P. Wigner, Z. Phys. 47, 631 (1928), reprinted in J. Schwinger, *Quantum Electrodynamics* (Dover, New York, 1958).
[13]D. Mattis, *The Theory of Magnetism* (Harper and Row, New York, 1965).
[14]We thank Michael Peskin for first pointing this out to us.
[15]The σ^z's are keeping track of Fermi statistics. The difference in the two diagrams, Fig. 8(a) and Fig. 8(b), comes from the relative minus sign between

$$\langle\Omega|\phi^\dagger_{\rho_2}(l+1)\phi_{\rho_1}(l+2)(\phi^\dagger_{\rho_1}(l+1)\phi^{\cdot\cdot}_{\rho_1}(l))(\phi^{\dagger\cdot\cdot}_{\rho_1}(l+2)\phi^{\cdot}_{\rho_1}(l+1))\phi^\dagger_{\rho_1}(l)\phi_{\rho_2}(l+1)|\Omega\rangle \quad (l=\text{even},\ \rho_1\neq\rho_2)$$

and

$$\langle\Omega|\phi^\dagger_{\rho'}(l+1)\phi_{\rho'}(l+2)(\phi^{\dagger\cdot}_{\rho}(l+1)\phi^{\cdot\cdot}_{\rho}(l))(\phi^\dagger_{\rho'}(l+2)\phi_{\rho'}(l+1))\phi^{\dagger\cdot\cdot}_{\rho}(l)\phi^{\cdot}_{\rho}(l+1)|\Omega\rangle \quad (l=\text{even},\ \rho\neq\rho').$$

[16]Instead of (2.21) we write

$$\sum_{\alpha=1}^{N}\bar\psi^c_\alpha\psi^c_\alpha\to\frac{\sum_\alpha^N\int\bar\psi^c_\alpha\psi^c_\alpha dz}{\int dz}$$

$$\to\frac{-\frac{1}{2}\sum_{l=1}^{L}\sum_\alpha^N\sigma^z_\alpha(l)}{La}.$$

[17]The fact that the gap depends on g^2 in a nonanalytic fashion in any asymptotically free theory was discussed and stressed by K. Lane, Phys. Rev. D 10, 1353 (1974); 10, 2605 (1974). It was also discussed in Ref. 5.
[18]See, for instance, A. L. Fetter and J. D. Walecka, *Quantum Theory of Many Particle Systems* (McGraw-Hill, New York, 1971).
[19]This is the result of Ref. 7. The dictionary needed consists of the following:

This paper		Zee's conventions
$(2N-1)$	→	$2N$
a	→	$a/2$
L	→	$2L$
g^2	→	g_0^2/N

[20]*Handbook of Mathematical Functions*, edited by M. Abramowitz and I. A. Stegun (Dover, New York, 1965).